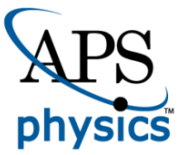

Theory of Deterministic Entanglement Generation between Remote Superconducting Atoms

K. Koshino, K. Inomata, Z. R. Lin, Y. Tokunaga, T. Yamamoto, and Y. Nakamura

Phys. Rev. Applied **7**, 064006 — Published 5 June 2017

DOI: 10.1103/PhysRevApplied.7.064006

Theory of deterministic entanglement generation between remote superconducting atoms

K. Koshino,[1] K. Inomata,[2,3] Z. R. Lin,[2] Y. Tokunaga,[4] T. Yamamoto,[5] and Y. Nakamura[2,6]

[1]*College of Liberal Arts and Sciences, Tokyo Medical and Dental University, Ichikawa, Chiba 272-0827, Japan*
[2]*RIKEN Center for Emergent Matter Science, Wako, Saitama 351-0198, Japan*
[3]*National Institute of Advanced Industrial Science and Technology, Tsukuba, Ibaraki 305-8563, Japan*
[4]*NTT Secure Platform Laboratories, NTT Corporation, Musashino 180-8585, Japan*
[5]*IoT Device Research Laboratories, NEC Corporation, Tsukuba, Ibaraki 305-8501, Japan*
[6]*Research Center for Advanced Science and Technology, The University of Tokyo, Meguro-ku, Tokyo 153-8904, Japan*

Entangling remote qubits is an essential technological element in the distributed quantum information processing. Here, we propose a deterministic scheme to generate maximal entanglement between remote superconducting atoms, using a propagating microwave photon as a flying qubit. The building block of this scheme is an atom-photon two-qubit gate, in which the photon qubit is encoded on its carrier frequencies. The gate operation completes deterministically upon reflection of a photon, and the gate type can be continuously varied (including SWAP, $\sqrt{\text{SWAP}}$, and Identity) through *in situ* control of the drive field. Applying such atom-photon gates sequentially, we can perform various gate operations between remote superconducting atoms.

I. INTRODUCTION

Physical implementation of scalable quantum information processing is one of the main objectives in modern quantum technology. There are two approaches for achieving this goal. In the first approach, we construct an integrated quantum circuit which is composed of qubits of the same kind: the one-qubit gates are realized by local operations on a single qubit, and the two-qubit gates are realized by mutual interaction between a pair of adjacent qubits. For example, high-fidelity gate operations reaching the fault tolerance threshold for surface code error correction [1] have been achieved in an array of superconducting qubits [2]. Recently, a scalable Shor's algorithm [3] has been demonstrated using a trapped ion quantum computer [4].

In the second approach, which is known as the distributed or modular architecture, we use a hybrid quantum network composed of flying and stationary qubits [5–10]. Flying qubits, which are typically implemented by photons, transfer quantum information among the stationary nodes. The stationary qubits, which are implemented by real or artificial atoms, are used to register and process quantum information. Construction of such hybrid quantum networks has been developed actively in cavity quantum electrodynamics (QED) using real atoms and optical photons. For example, a deterministic quantum gate between a propagating photon and an atom has been demonstrated, which has been further extended to a photon-photon gate [11–13]. The observation of single-photon Raman interaction [14, 15] would be a crucial step towards achieving the swap-based photon-photon gates [16]. Similarly, in the microwave quantum-optics setups based on circuit QED [17, 18], we can connect superconducting atoms by microwave photons propagating in waveguides. Recently, entanglement generation between two remote superconducting atoms has been achieved through the joint qubit-state measurement aided by a continuous field [19] or single photons [20] in the microwave domain. In both schemes, entanglement generation succeeds probabilistically, conditioned on a specific outcome of the joint measurement.

In this study, we propose a deterministic scheme for generating maximal entanglement between remote superconducting atoms, which is free from measurements on microwave photons. The building block of this scheme is a two-qubit gate between a superconducting atom and a propagating microwave photon. In this gate, a driven superconducting atom is coupled to a waveguide photon via a resonator (Fig. 1). The atomic qubit is encoded on its two lowest levels, and the photon qubit is encoded on its carrier frequencies [21]. The gate operation completes deterministically upon reflection of a photon, and the gate type is continuously variable (including SWAP, $\sqrt{\text{SWAP}}$, and Identity gates) through *in situ* control of the drive field to the atom. Using a propagating photon as a flying qubit, we can execute various gate operations between remote superconducting atoms, such as the entanglement generation and the qubit-state transfer. The present scheme provides a communication channel between distant clusters of superconducting qubits and thus widens the potential of quantum computation in superconducting devices.

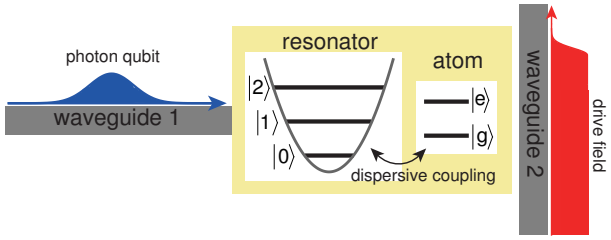

FIG. 1: Schematic of the tunable atom-photon quantum gate. We input a photon qubit through waveguide 1 and drive the superconducting atom through waveguide 2. The quantum-gate operation completes deterministically upon reflection of the photon. We can realize various types of quantum gate by changing the drive condition.

II. ATOM-PHOTON GATE

A. Setup

In this section, we discuss a two-qubit gate between a superconducting atom and a microwave photon propagating in a waveguide. The schematic of the considered device is shown in Fig. 1. A superconducting artificial atom, which can be regarded as a two-level system, is dispersively coupled to a resonator. The resonator and the atom are respectively coupled to waveguides 1 and 2. Through waveguide 1, we input a microwave-photon qubit, whose quantum information is encoded on its carrier frequencies. Through waveguide 2, we apply a drive field to the atom in order to engineer the dressed states of the atom-resonator system [22]. Assuming a static drive field of amplitude Ω_d and frequency ω_d, the Hamiltonian of the atom-resonator system is given, in the rotating frame, by

$$\mathcal{H}_{ar} = \omega_r a^\dagger a \sigma\sigma^\dagger + [(\omega_a-\omega_d)+(\omega_r-2\chi)a^\dagger a]\sigma^\dagger\sigma + \Omega_d(\sigma^\dagger+\sigma), \tag{1}$$

where σ (a) is the annihilation operator for the atom (resonator), ω_a (ω_r) is the resonance frequency of the atom (resonator), and χ is the dispersive shift. For concreteness, we assume the following parameter values: $\omega_a/2\pi = 5$ GHz, $\omega_r/2\pi = 10$ GHz, and $\chi/2\pi = 75$ MHz.

Throughout this study, we use the lowest four levels of the atom-resonator system, $|g,0\rangle$, $|e,0\rangle$, $|g,1\rangle$, and $|e,1\rangle$. These *bare* states are the eigenstates of $\mathcal{H}_{ar}$ when the drive field is off ($\Omega_d = 0$). We set the drive frequency ω_d within the range of $\omega_a - 2\chi < \omega_d < \omega_a$. Then, in the frame rotating at ω_d, we obtain a nested energy diagram of the bare states, where $\omega_{|g,0\rangle} < \omega_{|e,0\rangle} < \omega_{|e,1\rangle} < \omega_{|g,1\rangle}$. When the drive field is on, the bare states are hybridized to form the dressed states. We label them from the lowest in energy and denote them by $|\widetilde{1}\rangle$, $|\widetilde{2}\rangle$, $|\widetilde{3}\rangle$, and $|\widetilde{4}\rangle$ [Fig. 2(a)]. Diagonalizing $\mathcal{H}_{ar}$, they are given by

$$|\widetilde{1}\rangle = \cos\theta_l|g,0\rangle - \sin\theta_l|e,0\rangle, \tag{2}$$
$$|\widetilde{2}\rangle = \sin\theta_l|g,0\rangle + \cos\theta_l|e,0\rangle, \tag{3}$$
$$|\widetilde{3}\rangle = \cos\theta_h|e,1\rangle - \sin\theta_h|g,1\rangle, \tag{4}$$
$$|\widetilde{4}\rangle = \sin\theta_h|e,1\rangle + \cos\theta_h|g,1\rangle, \tag{5}$$

where $\theta_l = \frac{1}{2}\arg(\frac{\omega_a-\omega_d}{2} + i\Omega_d)$ and $\theta_h = \frac{1}{2}\arg(\frac{\omega_d-\omega_a+2\chi}{2} + i\Omega_d)$. Their eigenenergies are given by

$$\widetilde{\omega}_{1,2} = \tfrac{\omega_a-\omega_d}{2} \pm \sqrt{\left(\tfrac{\omega_a-\omega_d}{2}\right)^2+\Omega_d^2}, \tag{6}$$
$$\widetilde{\omega}_{3,4} = \omega_r - \tfrac{\omega_d-\omega_a+2\chi}{2} \pm \sqrt{\left(\tfrac{\omega_d-\omega_a+2\chi}{2}\right)^2+\Omega_d^2}, \tag{7}$$

where the plus (minus) sign is taken for $\widetilde{\omega}_2$ and $\widetilde{\omega}_4$ ($\widetilde{\omega}_1$ and $\widetilde{\omega}_3$). In this four level system, $|\widetilde{3}\rangle$ and $|\widetilde{4}\rangle$ decay to $|\widetilde{1}\rangle$ and $|\widetilde{2}\rangle$ emitting a photon into waveguide 1. Denoting the radiative decay rate of resonator by κ, the decay rates between the dressed states are given by

$$\widetilde{\kappa}_{32} = \widetilde{\kappa}_{41} = \kappa\cos^2\theta_t, \tag{8}$$
$$\widetilde{\kappa}_{31} = \widetilde{\kappa}_{42} = \kappa\sin^2\theta_t, \tag{9}$$

where $\theta_t = \theta_l + \theta_h$.

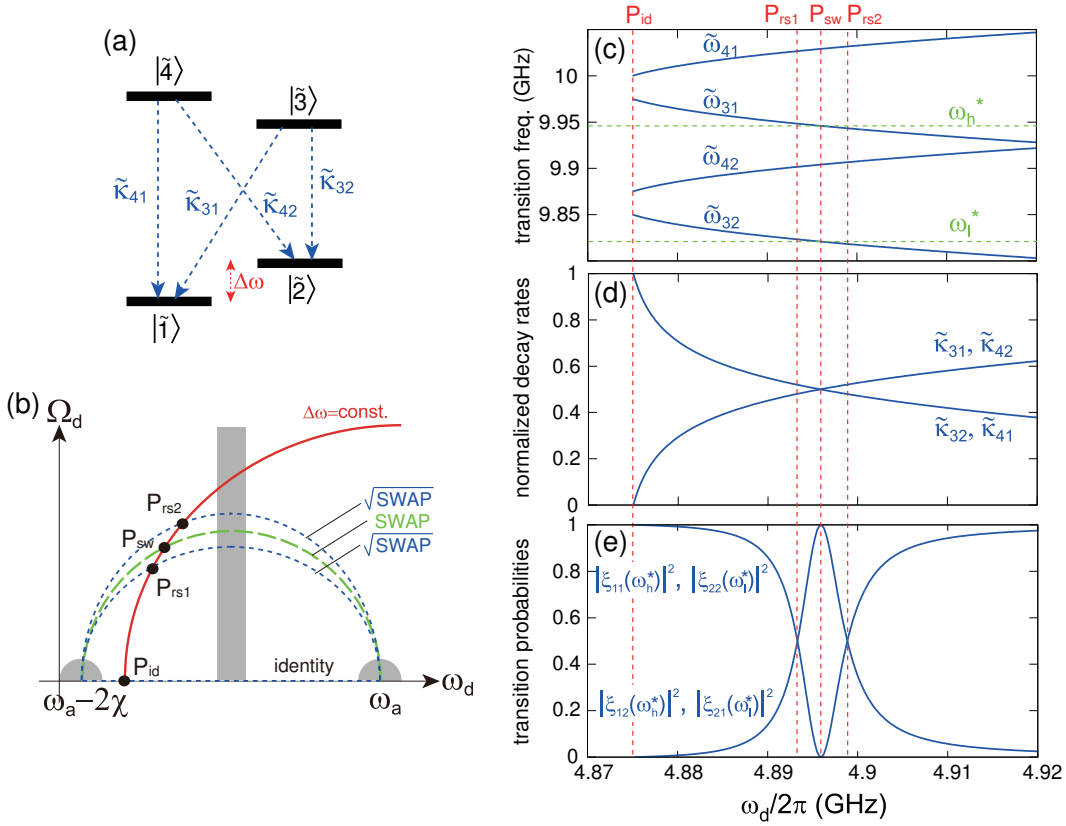

FIG. 2: Dressed-state engineering. (a) Level structure of the dressed states in the rotating frame. (b) Drive conditions to achieve various quantum gates. We change the drive condition along the red solid line, where $\Delta\omega = \widetilde{\omega}_{21}$ is kept constant. SWAP gate is realized at $\mathrm{P_{sw}}$, $\sqrt{\mathrm{SWAP}}$ is realized at $\mathrm{P_{rs1/2}}$, and Identity gate is realized at $\mathrm{P_{id}}$. In the shadowed areas, the gate fidelities are degraded due to the parasitic excitations. (c) Transition frequencies $\widetilde{\omega}_{ij}$, (d) normalized decay rates $\widetilde{\kappa}_{ij}/\kappa$, and (e) transition probabilities $|\xi_{ij}|^2$ as functions of ω_d. Ω_d is adjusted to satisfy $\Delta\omega/2\pi = 125$ MHz.

B. Single-photon response

We discuss the response of this four-level system to a single microwave photon input through waveguide 1. For simplicity, we assume that the input photon is monochromatic with frequency ω. Furthermore, we assume that both $|\widetilde{1}\rangle$ and $|\widetilde{2}\rangle$ are stable and the four-level system is in their superposition initially. Due to the oblique decay paths ($\widetilde{\kappa}_{31}$ and $\widetilde{\kappa}_{42}$), the input photon may induce the Raman transition upon reflection. The state vector of the overall system, consisting of a propagating photon and the dressed states, evolves as

$$|\widetilde{1},\omega\rangle \;\rightarrow\; \xi_{11}(\omega)|\widetilde{1},\omega\rangle + \xi_{12}(\omega)|\widetilde{2},\omega-\Delta\omega\rangle, \tag{10}$$

$$|\widetilde{2},\omega\rangle \;\rightarrow\; \xi_{21}(\omega)|\widetilde{1},\omega+\Delta\omega\rangle + \xi_{22}(\omega)|\widetilde{2},\omega\rangle, \tag{11}$$

where $\Delta\omega = \widetilde{\omega}_{21} = \widetilde{\omega}_2 - \widetilde{\omega}_1$. The coefficients ξ_{ij} are given by (see Appendix A)

$$\xi_{11}(\omega) = 1 - \frac{\kappa\sin^2\theta_t}{\frac{\kappa}{2} - i(\omega-\widetilde{\omega}_{31})} - \frac{\kappa\cos^2\theta_t}{\frac{\kappa}{2} - i(\omega-\widetilde{\omega}_{41})}, \tag{12}$$

$$\xi_{12}(\omega) = \frac{\kappa\sin\theta_t\cos\theta_t}{\frac{\kappa}{2} - i(\omega-\widetilde{\omega}_{31})} - \frac{\kappa\sin\theta_t\cos\theta_t}{\frac{\kappa}{2} - i(\omega-\widetilde{\omega}_{41})}, \tag{13}$$

$$\xi_{21}(\omega) = \frac{\kappa\sin\theta_t\cos\theta_t}{\frac{\kappa}{2} - i(\omega-\widetilde{\omega}_{32})} - \frac{\kappa\sin\theta_t\cos\theta_t}{\frac{\kappa}{2} - i(\omega-\widetilde{\omega}_{42})}, \tag{14}$$

$$\xi_{22}(\omega) = 1 - \frac{\kappa\cos^2\theta_t}{\frac{\kappa}{2} - i(\omega-\widetilde{\omega}_{32})} - \frac{\kappa\sin^2\theta_t}{\frac{\kappa}{2} - i(\omega-\widetilde{\omega}_{42})}. \tag{15}$$

We can confirm the probability conservation, $|\xi_{11}|^2 + |\xi_{12}|^2 = |\xi_{21}|^2 + |\xi_{22}|^2 = 1$.

C. SWAP gate

In the proposed atom-photon gate, we use $|\widetilde{1}\rangle$ and $|\widetilde{2}\rangle$ as the logical basis for the material node. Note that these states are roughly the atomic ground and excited states ($|\widetilde{1}\rangle \approx |g,0\rangle$ and $|\widetilde{2}\rangle \approx |e,0\rangle$) under our choice of the drive condition. For the photonic qubit, we encode quantum information on its career frequency: the basis states are $|\omega_l\rangle$ and $|\omega_h\rangle$, where $(\omega_l, \omega_h) = (\widetilde{\omega}_{32}, \widetilde{\omega}_{31})$ or $(\widetilde{\omega}_{42}, \widetilde{\omega}_{41})$. For concreteness, we focus on the former case and use $|\widetilde{1}\rangle$, $|\widetilde{2}\rangle$ and $|\widetilde{3}\rangle$ as a Λ system hereafter. The case of an "impedance-matched" Λ system, where $\theta_t = \pi/4$ and therefore $\widetilde{\kappa}_{31} = \widetilde{\kappa}_{32}$, is of particular importance. If $\omega_l (= \widetilde{\omega}_{32})$ is detuned sufficiently from the non-target transitions ($\widetilde{\omega}_{31}$, $\widetilde{\omega}_{41}$, and $\widetilde{\omega}_{42}$), we immediately observe in Eqs. (12)–(15) that $\xi_{11}(\omega_l) = \xi_{21}(\omega_l) = 1$ and $\xi_{12}(\omega_l) = \xi_{22}(\omega_l) = 0$, which implies that $|\widetilde{1}, \omega_l\rangle \to |\widetilde{1}, \omega_l\rangle$ and $|\widetilde{2}, \omega_l\rangle \to |\widetilde{1}, \omega_h\rangle$. Similarly, $|\widetilde{1}, \omega_h\rangle \to |\widetilde{2}, \omega_l\rangle$ and $|\widetilde{2}, \omega_h\rangle \to |\widetilde{2}, \omega_h\rangle$. These four time evolutions are summarized as

$$(\alpha_1|\widetilde{1}\rangle + \alpha_2|\widetilde{2}\rangle) \otimes (\beta_1|\omega_l\rangle + \beta_2|\omega_h\rangle) \to (\beta_1|\widetilde{1}\rangle + \beta_2|\widetilde{2}\rangle) \otimes (\alpha_1|\omega_l\rangle + \alpha_2|\omega_h\rangle). \tag{16}$$

where α_1, α_2, β_1 and β_2 are arbitrary coefficients. Namely, SWAP gate is achieved between the photon and atom qubits. Note that the deterministic Raman transition, $|\widetilde{1}, \omega_h\rangle \to |\widetilde{2}, \omega_l\rangle$, has been demonstrated recently as the deterministic down-conversion [22, 23] and is applied for detection of single microwave photons [24, 25].

The frequency ω_d and the amplitude Ω_d of the qubit drive are chosen as follows: (i) In order to constitute an impedance-matched Λ system ($\theta_t = \pi/4$), ω_d and Ω_d should satisfy

$$4\Omega_d^2 = (\omega_a - \omega_d)(\omega_d - \omega_a + 2\chi). \tag{17}$$

This is represented as an ellipse on the (ω_d, Ω_d) plane [green dashed line in Fig. 2(b)]. (ii) $\omega_l (= \widetilde{\omega}_{32})$ and $\omega_h (= \widetilde{\omega}_{31})$ should be detuned sufficiently from the non-target transitions. This requires that $(\omega_d, \Omega_d) \neq (\omega_a - 2\chi, 0)$, $(\omega_d, \Omega_d) \neq (\omega_a, 0)$, and $\omega_d \neq \omega_a - \chi$ [shadowed areas in Fig. 2(b)]. (iii) The frequency difference between the two basis states, $\Delta\omega = \omega_h - \omega_l$ is given, from Eq. (6), by

$$\Delta\omega = \sqrt{(\omega_a - \omega_d)^2 + 4\Omega_d^2}. \tag{18}$$

The condition that $\Delta\omega =$ constant is also represented as an ellipse on the (ω_d, Ω_d) plane [red solid line in Fig. 2(b)]. Practically, a large $\Delta\omega$ is advantageous, since we can suppress the effects of finite qubit lifetime by using a short photon pulse. Hereafter we set $\Delta\omega/2\pi = 125$ MHz. From Eqs. (17) and (18), the drive condition to achieve a SWAP gate is determined as

$$\omega_d^{\rm sw} = \omega_a - \tfrac{(\Delta\omega)^2}{2\chi}, \tag{19}$$

$$\Omega_d^{\rm sw} = \tfrac{\Delta\omega}{4\chi}\sqrt{4\chi^2 - (\Delta\omega)^2}, \tag{20}$$

which amount to $\omega_d^{\rm sw}/2\pi = 4.896$ GHz and $\Omega_d^{\rm sw}/2\pi = 34.55$ MHz, respectively [$\rm P_{sw}$ in Fig. 2(b)]. With this qubit drive, the carrier frequencies of the photon qubit are determined as

$$\omega_l^* = \omega_r - \chi - \sqrt{\chi^2 - (\tfrac{\Delta\omega}{2})^2} - \tfrac{\Delta\omega}{2}, \tag{21}$$

$$\omega_h^* = \omega_r - \chi - \sqrt{\chi^2 - (\tfrac{\Delta\omega}{2})^2} + \tfrac{\Delta\omega}{2}, \tag{22}$$

which amounts to $\omega_l^*/2\pi = 9.821$ GHz and $\omega_h^*/2\pi = 9.946$ GHz, respectively [Fig. 2(c)].

D. $\sqrt{\rm SWAP}$ and Identity gates

A merit of the present scheme is that the transition frequencies and the decay rates between the dressed states are controllable through the drive field. In particular, we can vary the drive condition conserving the frequency difference $\Delta\omega$ between $|\widetilde{1}\rangle$ and $|\widetilde{2}\rangle$ [solid line in Fig. 2(b)]. By changing the drive condition smoothly with a transit time of the order of 10 ns, we can suppress the non-adiabatic transition between $|\widetilde{1}\rangle$ and $|\widetilde{2}\rangle$. This implies that various atom-photon gates can be realized without changing the logical basis.

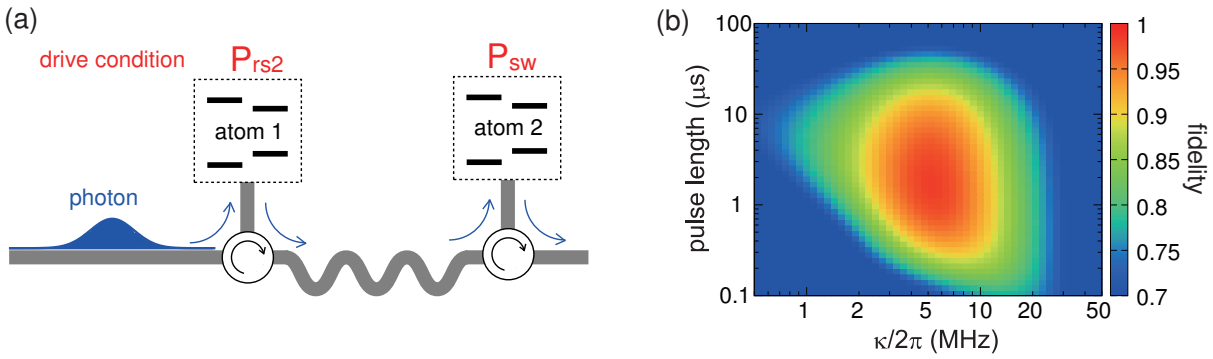

FIG. 3: Entanglement generation between remote superconducting atoms. (a) Schematic of the circuit. Superconducting atoms 1 and 2 are cascaded by circulators. Initially, both atoms are prepared to be in state $|\widetilde{1}\rangle$ and a single photon $|\omega_h^*\rangle$ is input. The drive conditions for atoms 1 and 2 are respectively set at $\mathrm{P_{rs2}}$ and $\mathrm{P_{sw}}$ of Fig. 2(b). (b) Fidelity of the generated entangled state as a function of the resonator linewidth κ and the pulse length l. The maximum fidelity of 0.983 is obtained by setting $\kappa/2\pi$ =5.482 MHz and $l = 1.584$ μs.

We observe in Fig. 2(c) that ω_l^* (ω_h^*) is always out of resonance with $\widetilde{\omega}_{31}$ and $\widetilde{\omega}_{41}$ ($\widetilde{\omega}_{32}$ and $\widetilde{\omega}_{42}$). Therefore, two of the basis states, $|\widetilde{1},\omega_l^*\rangle$ and $|\widetilde{2},\omega_h^*\rangle$, remain unchanged upon reflection of a photon regardless of the drive condition. In contrast, the dynamics of $|\widetilde{1},\omega_h^*\rangle$ and $|\widetilde{2},\omega_l^*\rangle$ are highly sensitive to the drive condition. To observe this, we show the drive-frequency dependence of $|\xi_{11}(\omega_h^*)|^2$, $|\xi_{12}(\omega_h^*)|^2$, $|\xi_{21}(\omega_l^*)|^2$, and $|\xi_{22}(\omega_l^*)|^2$ in Fig. 2(e). Note that $|\xi_{11}(\omega_h^*)|^2 = |\xi_{22}(\omega_l^*)|^2$ and $|\xi_{12}(\omega_h^*)|^2 = |\xi_{21}(\omega_l^*)|^2$ in this plot. As we discussed in Sec. II C, $|\xi_{12}(\omega_h^*)|^2$ and $|\xi_{21}(\omega_l^*)|^2$ take their maximal value of unity under the drive condition of SWAP gate [$\mathrm{P_{sw}}$ in Fig. 2(b)–(e)]. In contrast, when the qubit drive is off, $|\xi_{12}(\omega_h^*)|^2$ and $|\xi_{21}(\omega_l^*)|^2$ take their minimal value of zero [$\mathrm{P_{id}}$ of Fig. 2(b)–(e)]. Then we realize an Identity gate, where both of the atom and the photon qubits remain unchanged upon reflection. Another important operation mode is a $\sqrt{\mathrm{SWAP}}$ gate, which generates maximal entanglement between the atom and photon qubits [26]. This is realized at $\mathrm{P_{rs1}}$ and $\mathrm{P_{rs2}}$ of Fig. 2(b)–(e), where $|\xi_{11}(\omega_h^*)|^2 = |\xi_{12}(\omega_h^*)|^2 = |\xi_{21}(\omega_l^*)|^2 = |\xi_{22}(\omega_l^*)|^2 = 1/2$. The basis states evolve as

$$|\widetilde{1},\omega_l^*\rangle \rightarrow |\widetilde{1},\omega_l^*\rangle, \tag{23}$$
$$|\widetilde{1},\omega_h^*\rangle \rightarrow \tfrac{1\mp i}{2}|\widetilde{1},\omega_h^*\rangle + \tfrac{1\pm i}{2}|\widetilde{2},\omega_l^*\rangle, \tag{24}$$
$$|\widetilde{2},\omega_l^*\rangle \rightarrow \tfrac{1\pm i}{2}|\widetilde{1},\omega_h^*\rangle + \tfrac{1\mp i}{2}|\widetilde{2},\omega_l^*\rangle, \tag{25}$$
$$|\widetilde{2},\omega_h^*\rangle \rightarrow |\widetilde{2},\omega_h^*\rangle, \tag{26}$$

where the upper (lower) signs should be taken at $\mathrm{P_{rs1}}$ ($\mathrm{P_{rs2}}$). The drive conditions are $\omega_d^{\mathrm{rs1}}/2\pi = 4.893$ GHz and $\Omega_d^{\mathrm{rs1}}/2\pi = 32.46$ MHz at $\mathrm{P_{rs1}}$, and $\omega_d^{\mathrm{rs2}}/2\pi = 4.899$ GHz and $\Omega_d^{\mathrm{rs2}}/2\pi = 36.60$ MHz at $\mathrm{P_{rs2}}$.

III. ENTANGLEMENT GENERATION BETWEEN REMOTE ATOMS

A. Evolution of atom–atom–photon system

By cascading such atom-resonator systems using circulators, we can construct a one-dimensional network of atomic qubits which are connected quantum-mechanically by flying qubits, and perform various gate operations between remote qubits. As an application of practical importance, we here discuss a deterministic entangler of two remote superconducting atoms, which is essential for distributed quantum information processing.

We consider a system of two remote superconducting atoms connected by a microwave transmission line, as depicted in Fig. 3(a). Initially, both atoms are in the ground state $|g\rangle$. We adiabatically switch on the drive fields to the atoms: the drive condition is $\mathrm{P_{rs2}}$ of Fig. 2(b) for atom 1 and $\mathrm{P_{sw}}$ for atom 2. After adiabatic switching on of the drive fields, which typically takes several tens of nanoseconds [24, 25], both atoms are in state $|\widetilde{1}\rangle$. Then, we input a single photon $|\omega_h^*\rangle$ into this circuit. The state vector of the overall system (atom 1, 2, and photon) is written as $|\widetilde{1}\rangle_1 \otimes |\widetilde{1}\rangle_2 \otimes |\omega_h^*\rangle_p \equiv |\widetilde{1},\widetilde{1},\omega_h^*\rangle$. After reflection of the photon at atom 1, a $\sqrt{\mathrm{SWAP}}$ gate is applied to atom 1 and the

photon. According to Eq. (24), the state vector evolves as

$$|\widetilde{1},\widetilde{1},\omega_h^*\rangle \to \tfrac{1+i}{2}|\widetilde{1},\widetilde{1},\omega_h^*\rangle + \tfrac{1-i}{2}|\widetilde{2},\widetilde{1},\omega_l^*\rangle. \tag{27}$$

After reflection of the photon at atom 2, a SWAP gate is applied to atom 2 and the photon. According to Eq. (16), the state vector further evolves as

$$\to \left(\tfrac{1+i}{2}|\widetilde{1},\widetilde{2}\rangle + \tfrac{1-i}{2}|\widetilde{2},\widetilde{1}\rangle\right) \otimes |\omega_l^*\rangle. \tag{28}$$

Finally, by adiabatically switching off the drive fields, we obtain a maximally entangled state of remote qubits, $\frac{1+i}{2}|g,e\rangle + \frac{1-i}{2}|e,g\rangle$. Note that, in the final state of Eq. (28), the photon is disentangled from both atoms. Therefore, the present scheme completes deterministically, without the need for measurement on the output microwave photons.

B. Fidelity

In the above discussions, the lifetime T_1 of the superconducting atom and the length l of the photon pulse are assumed to be infinite. Here, taking account of their finiteness, we quantitatively evaluate the fidelity of the generated entangled state. We assume a long-lived superconducting atom with $T_1 = 80$ μs and with negligible pure dephasing, and employ a trigonometric pulse profile for the photon qubit, as given by

$$f_{\omega,l}(t) = \begin{cases} \sqrt{2/l}\cos(\pi t/l)\exp(-i\omega t) & (|t| < l/2) \\ 0 & (\text{otherwise}) \end{cases}, \tag{29}$$

where l is the pulse length and $\omega(=\omega_l^*,\omega_h^*)$ is the center frequency. For $\Delta\omega/2\pi = 125$ MHz, the two basis states $|\omega_h^*\rangle$ and $|\omega_l^*\rangle$ are almost orthogonal ($|\langle\omega_l^*|\omega_h^*\rangle| \lesssim 10^{-3}$) for $l \gtrsim 50$ ns. Note that a pulse-shaped single photon is available in the microwave domain [27].

Typically, the propagation time between the superconducting atoms is much shorter than the pulse length of the input photon. Therefore, we can safely regard the pulse length l as the gate time. Setting the initial moment at $t = -l/2$, we evaluate the fidelity of the generated two-qubit entangled state after photon reflection at $t = l/2$. In Fig. 3(b), the fidelity is plotted as a function of κ and l (see Appendix B for calculation details). The conditions for high-fidelity entanglement generation are as follows: (i) The gate time l is much shorter than the lifetime T_1 of the atom. (ii) In atom-photon gates, the photon pulse is generally delayed due to absorption and reemission by the atom and degrades the fidelity. Therefore, the pulse length l should be much larger than the delay time ($\sim \kappa^{-1}$) so that such delay becomes negligible. (iii) Levels $|\widetilde{3}\rangle$ and $|\widetilde{4}\rangle$ are well resolved in frequency, which requires $\kappa \ll \widetilde{\omega}_{43} \simeq 2\pi \times 70$ MHz [see Fig. 2(c)].

The fidelity of the generated entangled state is plotted in Fig. 3(b) as a function of the resonator linewidth κ and the pulse length l. By setting $\kappa/2\pi = 5.482$ MHz and $l = 1.584$ μs, the fidelity of the generated entangled state reach 0.983. This is sufficient for the communication channel in the distributed quantum information processing [8]. We can further improve this fidelity by enhancing the lifetime T_1 of the atom. Alternately, we can improve the fidelity by enhancing the dispersive shift χ and the cavity linewidth κ, which enables the use of a shorter photon pulse.

C. Tunability of operation mode

An advantage of the present scheme is that the operation mode can be controlled *in situ* through the atomic drive, without changing the circuit configuration nor the carrier frequencies ω_l^* and ω_h^* of the photonic qubits. For example, by setting the drive condition of atom 1 at $\mathrm{P_{rs1}}$, we obtain a maximal entangled state of $\frac{1-i}{2}|g,e\rangle + \frac{1+i}{2}|e,g\rangle$. Thus, we can control the relative phase of superposition.

Another operation mode of practical importance is the deterministic qubit-state transfer between remote atoms. For this purpose, we set the drive conditions of both atoms at $\mathrm{P_{sw}}$, and send a single photon tuned to $|\omega_l^*\rangle$ or $|\omega_h^*\rangle$ (or their arbitrary superposition). This deterministically transfers the qubit stored in atom 1 to atom 2; the input photon qubit is transferred to atom 1, and the qubit stored in atom 2 is transferred to the output photon. If three or more superconducting atoms are cascaded, the input photon induces a quantum domino, in which the atomic qubits are successively transferred to the subsequent ones.

IV. SUMMARY

In summary, we theoretically proposed a two-qubit gate between a superconducting atom and a propagating microwave photon. The gate operation completes deterministically upon reflection of the photon, and various two-qubit gates (including SWAP, $\sqrt{\text{SWAP}}$, and Identity) are realizable through *in situ* control of the drive field. Applying this atom-photon gates successively, we can perform various gate operations between remote superconducting atoms. For example, we can deterministically generate maximum entanglement between two atoms using a microwave photon as a flying qubit. This opens the way for deterministic and quantum-mechanical connection between remote clusters of superconducting qubits and thus widens the potential of superconducting quantum computing.

Acknowledgments

This work was partly supported by JSPS KAKENHI (Grants No. 16K05497, No. 26220601, and No. 15K17731) and JST ERATO (Grant No. JPMJER1601).

Appendix A: Derivation of $\xi_{ij}(\omega)$

Here, we derive the coefficients $\xi_{ij}(\omega)$ which appear in Eqs. (12)–(15). The Hamiltonian of the overall system including waveguide 1 is given by

$$\mathcal{H} = \mathcal{H}_{ar} + \mathcal{H}_{rw}, \tag{A1}$$

$$\mathcal{H}_{ar} = \omega_r a^\dagger a \sigma\sigma^\dagger + [(\omega_q - \omega_d) + (\omega_r - 2\chi)a^\dagger a]\sigma^\dagger\sigma + \Omega_d(\sigma^\dagger + \sigma), \tag{A2}$$

$$\mathcal{H}_{rw} = \int dk \left[k a_k^\dagger a_k + \sqrt{\kappa/2\pi}(a^\dagger a_k + a_k^\dagger a)\right], \tag{A3}$$

where $\mathcal{H}_{ar}$ describes the driven atom-resonator system [Eq. (1)], $\mathcal{H}_{rw}$ describes the interaction between the resonator and the propagating photon in waveguide 1, and a_k is the annihilation operator of the waveguide photon with wave number k. The superconducting atom is assumed to have an infinite lifetime here. Switching to the dressed-state basis [Eqs. (2)–(5)], $\mathcal{H}$ is rewritten as

$$\mathcal{H} = \sum_j \widetilde{\omega}_j \sigma_{jj} + \int dk \left[k a_k^\dagger a_k + \textstyle\sum_{i,j}(\eta_{ji}\sigma_{ji}a_k + \eta_{ji}^* a_k^\dagger \sigma_{ij})/\sqrt{2\pi}\right], \tag{A4}$$

where the indices run over $i, j = 1, \cdots, 4$ and $\sigma_{ji} = |\widetilde{j}\rangle\langle\widetilde{i}|$. η_{ji} is given by $\eta_{32} = \eta_{41} = \sqrt{\kappa}\cos\theta_t$, $\eta_{42} = -\eta_{31} = \sqrt{\kappa}\sin\theta_t$, and $\eta_{ji} = 0$ otherwise.

We introduce the real-space representation of the field operator by $a_r = (2\pi)^{-1/2}\int dk\, e^{ikr} a_k$. In this representation, the $r < 0$ ($r > 0$) region corresponds to the incoming (outgoing) field. From Eq. (A4), we can rigorously derive the following input-output relation,

$$a_r(t) = a_{r-t}(0) - i\theta(r)\theta(t-r)\sum_{i,j}\eta_{ji}^*\sigma_{ij}(t-r), \tag{A5}$$

where $\theta(r)$ is the Heaviside step function. We can also derive the following Heisenberg equations,

$$\frac{d}{dt}\sigma_{13} = (-i\widetilde{\omega}_{31} - \kappa/2)\,\sigma_{13} + i[\eta_{31}(\sigma_{33} - \sigma_{11}) - \eta_{32}\sigma_{12} + \eta_{41}\sigma_{43}]a_{-t}(0), \tag{A6}$$

$$\frac{d}{dt}\sigma_{14} = (-i\widetilde{\omega}_{41} - \kappa/2)\,\sigma_{14} + i[\eta_{41}(\sigma_{44} - \sigma_{11}) - \eta_{42}\sigma_{12} + \eta_{31}\sigma_{34}]a_{-t}(0), \tag{A7}$$

where $\widetilde{\omega}_{ij} = \widetilde{\omega}_i - \widetilde{\omega}_j$.

Hereafter, we consider a case in which the atom is in the state $|\widetilde{1}\rangle$ and a single photon with wavefunction $f(r)$ is input at the initial moment ($t = 0$). The initial and final state vectors are written as

$$|\phi_{in}\rangle = \int dr f(r) a_r^\dagger |\widetilde{1}\rangle, \tag{A8}$$

$$|\phi_{out}\rangle = e^{-i\widetilde{\omega}_1 t}\int dr g_{11}(r,t) a_r^\dagger|\widetilde{1}\rangle + e^{-i\widetilde{\omega}_2 t}\int dr g_{12}(r,t) a_r^\dagger|\widetilde{2}\rangle, \tag{A9}$$

where $g_{11}(r,t)$ and $g_{12}(r,t)$ are the photon wavefunctions after reflection, and the final moment t is sufficiently large. The initial and final state vectors are connected by the unitary time evolution, $|\phi_{out}\rangle = e^{-i\mathcal{H}t}|\phi_{in}\rangle$. Note that the natural time evolution of the dressed state ($e^{-i\widetilde{\omega}_j t}$) is separated. For later convenience, we introduce $s_{13}(t) = \langle\widetilde{1}|\sigma_{13}(t)|\phi_{in}\rangle$ and $s_{14}(t) = \langle\widetilde{1}|\sigma_{14}(t)|\phi_{in}\rangle$. Their equations of motion are given, remembering that $a_{-t}(0)|\phi_{in}\rangle = f(-t)|\widetilde{1}\rangle$ and that $|\widetilde{1}\rangle$ is an eigenstate of $\mathcal{H}$, by

$$\frac{d}{dt}s_{13} = (-i\widetilde{\omega}_{31} - \kappa/2)s_{13} - i\eta_{31}f(-t), \tag{A10}$$

$$\frac{d}{dt}s_{14} = (-i\widetilde{\omega}_{41} - \kappa/2)s_{14} - i\eta_{41}f(-t). \tag{A11}$$

If the pulse length of the input photon is much larger than κ^{-1}, we can adiabatically solve the above equations. Denoting the central frequency of the input photon by ω, the adiabatic solutions are given by

$$s_{13}(t) = \frac{-i\eta_{31}}{\kappa/2 - i(\omega - \widetilde{\omega}_{31})}f(-t), \tag{A12}$$

$$s_{14}(t) = \frac{-i\eta_{41}}{\kappa/2 - i(\omega - \widetilde{\omega}_{41})}f(-t). \tag{A13}$$

From Eq. (A9), we have $g_{11}(r,t) = e^{i\widetilde{\omega}_1 t}\langle\widetilde{1}|a_r|\phi_{out}\rangle = \langle\widetilde{1}|a_r(t)|\phi_{in}\rangle$. Substituting Eq. (A5) into this equation, we obtain

$$\xi_{11}(\omega) = \frac{g_{11}(r,t)}{f(r-t)} = 1 - \frac{\kappa\sin^2\theta_t}{\kappa/2 - i(\omega - \widetilde{\omega}_{31})} - \frac{\kappa\cos^2\theta_t}{\kappa/2 - i(\omega - \widetilde{\omega}_{41})}. \tag{A14}$$

Thus, $\xi_{11}(\omega)$ [Eq. (12)] is derived. ξ_{12}, ξ_{21} and ξ_{22} are derivable similarly.

Appendix B: Fidelity of the generated entangled state

Here, we present the formalism for evaluation of the fidelity of the generated entangled state. Considering the finite pulse length of the input pulse, the input state vector is written as

$$|\widetilde{1},\widetilde{1},\omega_h^*\rangle = \int d\omega f_{\omega_h^*}(\omega)|\widetilde{1},\widetilde{1},\omega\rangle, \tag{B1}$$

where $f_{\omega_h^*}(\omega)$ is the wavefunction of the input photon in the frequency space. It is given, as the Fourier transform of Eq. (29) with $\omega = \omega_h^*$, by

$$f_{\omega_h^*}(\omega) = \sqrt{\frac{4\pi}{l^3}}\frac{1}{(\pi/l)^2 - (\omega - \omega_h^*)^2}\cos[(\omega - \omega_h^*)l/2], \tag{B2}$$

where l denotes the pulse length.

Upon reflection of the photon at the atom-resonator system, the state vector evolves as Eqs. (10)–(11). Considering that the drive condition of atom 1 (2) is set at $\mathrm{P_{rs2}}$ ($\mathrm{P_{sw}}$), the state vector after second reflection is written as $\sum_{i,j=1,2}\int d\omega m_{ij}(\omega)|\widetilde{i},\widetilde{j},\omega\rangle$, where

$$m_{11}(\omega) = f_{\omega_h^*}(\omega)\xi_{11}^{\mathrm{rs2}}(\omega)\xi_{11}^{\mathrm{sw}}(\omega), \tag{B3}$$

$$m_{12}(\omega) = f_{\omega_h^*}(\omega+\Delta\omega)\xi_{11}^{\mathrm{rs2}}(\omega+\Delta\omega)\xi_{12}^{\mathrm{sw}}(\omega+\Delta\omega), \tag{B4}$$

$$m_{21}(\omega) = f_{\omega_h^*}(\omega+\Delta\omega)\xi_{12}^{\mathrm{rs2}}(\omega+\Delta\omega)\xi_{11}^{\mathrm{sw}}(\omega), \tag{B5}$$

$$m_{22}(\omega) = f_{\omega_h^*}(\omega+2\Delta\omega)\xi_{12}^{\mathrm{rs2}}(\omega+2\Delta\omega)\xi_{12}^{\mathrm{sw}}(\omega+\Delta\omega). \tag{B6}$$

We also consider here the decay of the atomic excited state $|e\rangle$ during the gate time t_g. Using Eqs. (2) and (3), and denoting the atomic lifetime by T_1, the dressed states $|\widetilde{1}\rangle$ and $|\widetilde{2}\rangle$ evolve as

$$|\widetilde{1}\rangle \rightarrow |\widetilde{1}'\rangle = \cos\theta_l|g,0\rangle - e^{-t_g/2T_1}\sin\theta_l|e,0\rangle + \cdots, \tag{B7}$$

$$|\widetilde{2}\rangle \rightarrow |\widetilde{2}'\rangle = \sin\theta_l|g,0\rangle + e^{-t_g/2T_1}\cos\theta_l|e,0\rangle + \cdots, \tag{B8}$$

where the dots denote the decayed states, which are entangled with the environment and are out of the considered Hilbert space. The density matrix ρ of atoms 1 and 2 is then written as

$$\rho = \sum_{i,j} \sum_{k,l} \left[\int d\omega \; m_{ij}(\omega) m^*_{kl}(\omega) \right] |\widetilde{i}', \widetilde{j}'\rangle\langle \widetilde{k}', \widetilde{l}'|. \tag{B9}$$

On the other hand, from Eq. (28), the target entangled state is $|\psi_t\rangle = \frac{1+i}{2}|\widetilde{1}, \widetilde{2}\rangle + \frac{1-i}{2}|\widetilde{2}, \widetilde{1}\rangle$. The fidelity of the generated entangled state $\mathcal{F}$ is given by

$$\mathcal{F} = \sqrt{\langle\psi_t|\rho|\psi_t\rangle}. \tag{B10}$$

The fidelity thus calculated in shown in Fig. 3(b).

Practically, there exists finite photon loss in conventional circulators. When a photon passes a circulator once, the state vector evolves as $|\psi\rangle \to \sqrt{P_{tr}}|\psi\rangle + \sqrt{1-P_{tr}}|\psi'\rangle$, where P_{tr} is the photon transmission probability, $|\psi\rangle$ is the initial state, and $|\psi'\rangle$ is the state with photon loss. Note that $|\psi'\rangle$ is entangled with the environment and does not contribute to the fidelity. Considering that a photon qubit passes the circulators four times in the proposed scheme [Fig. 3(a)], the fidelity should be modified as $\mathcal{F} \to P_{tr}^4 \mathcal{F}$. Thus, the maximum fidelity 0.983 reached under the optimal condition ($\kappa/2\pi = 5.482$ MHz and $l = 1.584$ μs) is degraded to be 0.896 (0.620), when the photon loss per one passage through a circulator is 0.1 dB (0.5 dB). However, we would like to remind that the high fidelity presented in Fig. 3(b) can be recovered by detecting a microwave photon at the end of the circuit and using the present scheme as a *heralded* one. For this purpose, an input single photon can be replaced with a weak classical pulse with the mean photon number much less than unity.

[1] A. G. Fowler, M. Mariantoni, J. M. Martinis, and A. N. Cleland, *Surface codes: Towards practical large-scale quantum computation*, Phys. Rev. A **86**, 032324 (2012).

[2] R. Barends, J. Kelly, A. Megrant, A. Veitia *et al.*, *Logic gates at the surface code threshold: Superconducting qubits poised for fault-tolerant quantum computing*, Nature **508**, 500 (2014).

[3] A. Yu. Kitaev, *Quantum measurements and the Abelian stabilizer problem*, arXiv:quant-ph/9511026.

[4] T. Monz, D. Nigg, E. A. Martinez, M. F. Brandl, P. Schindler, R. Rines, S. X. Wang, I. L. Chuang, and R. Blatt, *Realization of a scalable Shor algorithm*, Science **351**, 1068 (2016).

[5] J. I. Cirac, A. K. Ekert, S. F. Huelga, and C. Macchiavello, *Distributed quantum computation over noisy channels*, Phys. Rev. A **59**, 4249 (1999).

[6] A. Serafini, S. Mancini, and S. Bose, *Distributed Quantum Computation via Optical Fibers*, Phys. Rev. Lett. **96**, 010503 (2006).

[7] H. J. Kimble, *The Quantum Internet*, Nature, **453**, 1023 (2008).

[8] N. H. Nickerson, Y. Li, and S. C. Benjamin, *Topological quantum computing with a very noisy network and local error rates approaching one percent*, Nat. Commun. **4**, 1756 (2013).

[9] C. Monroe, R. Raussendorf, A. Ruthven, K. R. Brown, P. Maunz, L.-M. Duan, and J. Kim, *Large-scale modular quantum-computer architecture with atomic memory and photonic interconnects*, Phys. Rev. A **89**, 022317 (2014).

[10] S. Debnath, N. M. Linke, C. Figgatt, K. A. Landsman, K. Wright, C. Monroe, *Demonstration of a small programmable quantum computer with atomic qubits*, Nature **536**, 63 (2016).

[11] L. M. Duan and H. J. Kimble, *Scalable Photonic Quantum Computation through Cavity-Assisted Interactions*, Phys. Rev. Lett. **92**, 127902 (2004).

[12] A. Reiserer and G. Rempe, *Cavity-based quantum networks with single atoms and optical photons*, Rev. Mod. Phys. **87**, 1379 (2015).

[13] B. Hacker, S. Welte, G. Rempe, and S. Ritter, *A photon-photon quantum gate based on a single atom in an optical resonator*, Nature **536**, 193 (2016).

[14] D. Pinotsi and A. Imamoglu, *Single Photon Absorption by a Single Quantum Emitter*, Phys. Rev. Lett. **100**, 093603 (2008).

[15] I. Shomroni, S. Rosenblum, Y. Lovsky, O. Bechler, G. Guendelman, and B. Dayan, *All-optical routing of single photons by a one-atom switch controlled by a single photon*, Science **345**, 903 (2014).

[16] K. Koshino, S. Ishizaka, and Y. Nakamura, *Deterministic photon-photon* $\sqrt{\text{SWAP}}$ *gate using a* Λ *system*, Phys. Rev. A **82**, 010301(R) (2010).

[17] A. Blais, R.-S. Huang, A. Wallraff, S. M. Girvin, and R. J. Schoelkopf, *Cavity quantum electrodynamics for superconducting electrical circuits: An architecture for quantum computation*, Phys. Rev. A **69**, 062320 (2004).

[18] A. Wallraff, D. I. Schuster, A. Blais, L. Frunzio, R.-S. Huang, J. Majer, S. Kumar, S. M. Girvin, and R. J. Schoelkopf, *Strong coupling of a single photon to a superconducting qubit using circuit quantum electrodynamics*, Nature **431**, 162 (2004).

[19] N. Roch, M. E. Schwartz, F. Motzoi, C. Macklin, R. Vijay, A. W. Eddins, A. N. Korotkov, K. B. Whaley, M. Sarovar, and I. Siddiqi, *Observation of Measurement-Induced Entanglement and Quantum Trajectories of Remote Superconducting Qubits*, Phys. Rev. Lett. **112**, 170501 (2014).

[20] A. Narla, S. Shankar, M. Hatridge, Z. Leghtas, K. M. Sliwa, E. Zalys-Geller, S. O. Mundhada, W. Pfaff, L. Frunzio, R. J. Schoelkopf, and M. H. Devoret, *Robust concurrent remote entanglement between two superconducting qubits*, Phys. Rev. X **6**, 031036 (2016).

[21] D. L. Moehring, P. Maunz, S. Olmschenk, K. C. Younge, D. N. Matsukevich, L.-M. Duan, and C. Monroe, *Entanglement of single-atom quantum bits at a distance*, Nature **449**, 68 (2007).

[22] K. Koshino, K. Inomata, T. Yamamoto and Y. Nakamura, *Implementation of an Impedance-Matched* Λ *System by Dressed-State Engineering*, Phys. Rev. Lett. **111**, 153601 (2013).

[23] K. Inomata, K. Koshino, Z. R. Lin, W. D. Oliver, J. S. Tsai, Y. Nakamura and T. Yamamoto, *Microwave Down-Conversion with an Impedance-Matched* Λ *System in Driven Circuit QED*, Phys. Rev. Lett. **113**, 063604 (2014).

[24] K. Koshino, K. Inomata, Z. Lin, Y. Nakamura and T. Yamamoto, *Theory of microwave single-photon detection using an impedance-matched* Λ *system*, Phys. Rev. A **91**, 043805 (2015).

[25] K. Inomata, Z. R. Lin, K. Koshino, W. D. Oliver, J. S. Tsai, T. Yamamoto, and Y. Nakamura, *Single microwave-photon detector using an artificial* Λ*-type three-level system*, Nat. Commun. **7**, 12303 (2016).

[26] D. Loss and D. P. DiVincenzo, *Quantum computation with quantum dots*, Phys. Rev. A **57**, 120 (1998).

[27] M. Pechal, L. Huthmacher, C. Eichler, S. Zeytinoglu, A. A. Abdumalikov, Jr., S. Berger, A. Wallraff, and S. Filipp, *Microwave-Controlled Generation of Shaped Single Photons in Circuit Quantum Electrodynamics*, Phys. Rev. X **4**, 041010 (2014).